Honors College

5-2012

Data Logging Radiation Detector

Joseph P. Record

Recommended Citation

DATA LOGGING RADIATION DETECTOR

by

Joseph P. Record

A Thesis Submitted in Partial Fulfillment
of the Requirements for a Degree with Honors
(Electrical Engineering)

The Honors College

University of Maine

May 2012

Advisory Committee:
    Richard Eason, Associate Professor of Electrical and Computer Engineering, Advisor
    Nuri Emanetoglu, Assistant Professor of Electrical and Computer Engineering
    Mark Haggerty, Rezendes Preceptor for Civic Engagement
    David Kotecki, Associate Professor of Electrical and Computer Engineering
    John Vetelino, Professor of Electrical and Computer Engineering

DATA LOGGING RADIATION DETECTOR

By Joseph P. Record

Thesis Advisor: Dr. Richard Eason

A Thesis Submitted in Partial Fulfillment
of the Requirements for a Degree with Honors
(Electrical Engineering)
May 2012

This thesis describes significance of radiation detection and describes the design, build, and test of a radiation detection device called the Data Logging Radiation Detector. The device is capable of measuring alpha, beta, and gamma radiation and storing the resulting data to an SD card. The Data Logging Radiation detector consists of four major blocks: a DC-DC boost switched mode power supply, a Geiger-Müller tube, an ATMega328p microcontroller, and a removable SD card. The switched mode power supply generates the necessary high voltage to bias the Geiger tube. Alpha particles, beta particles, and gamma rays are then able to be sensed when they collide with the tube, resulting in a pulse of current from the tube that can be processed by the microcontroller. The microcontroller then writes the data in counts per minute (CPM) to an SD card. The switching power supply achieved an output voltage of 514 V and 71% efficiency. Mean CPM data agree with a commercial Geiger counter to within 5%. Results are discussed and potential improvements suggested.

ACKNOWLEDGMENTS

TABLE OF CONTENTS

LIST OF TABLES

LIST OF FIGURES

Chapter 1

INTRODUCTION

This thesis presents background information into the theory and importance of radiation dectection, specifically focusing on the design and test of a radiation detection device called the Data Logging Radiation Dector. This device is a consumer level Geiger counter that is capable of measuring ionizing radiation which can be harmful to human health.

1.1 Overview

Geiger counters are able to sense the three types of ionizing radiation: alpha particles, beta particles, and gamma rays via a Geiger tube—a physical component that converts a radiation detection into an electrical signal. To power the Geiger tube, a switching power supply is implemented to boost a 5 V DC signal to a desired 550 V DC signal, suitable for the Geiger tube selected for this design. Once this high potential is placed across the two terminals of the Geiger tube, incoming alpha, beta, or gamma radiation will produce a pulse of current from the tube. This current, referred to as a count, is then processed by a microcontroller and stored in units of counts per minute (CPM) to removable memory in the form of an SD card. This enables a user to remotely sense radiation levels—something most commercial Geiger counters are unable to do.

1.2 Motivation

The motivation for this thesis was the Fukushima nuclear disaster of March 2011. The tsunami and following nuclear meltdown was a national tragedy for Japan. As a result, the Fukushima story garnered much global attention. This thesis describes the current state of nuclear power production using the Fukushima disaster as a example of

what went wrong and describes how a consumer device such as the Data Logging Radiation Detector could be used to prevent unnecessary harm to victims of future nuclear disasters.

1.3 Report Organization

Chapter 2 describes the implications and importance of being able to measuring radiation. Particular focus is given to the dangers of nuclear radiation, the demand for radiation measurement devices, and the governmental response following the Fukushima disaster. A design for the Data Logging Radiation dector is proposed.

The remaining chapters describe the analysis, design, construction, and test of the Data Logging Radiation Detector (this work was done in conjection with ECE capstone project partner Brian Grant). Chapter 3 focuses on the four major blocks of the Data Logging Radiation Detector and how these blocks achieve the desired goal of measuring radiation. Chapter 4 focuses on the design of the device including operation and implementation. Chapters 5 and 6 present experimental results and conclusions, respectively. Appendices are provided at the end of this thesis.

Chapter 2

BACKGROUND INFORMATION

The Japanese nuclear disaster of March 2011 highlighted inherent dangers with nuclear power generation, showed that demand for radiation detection was greater than supply, and exposed flaws in governmental response to nuclear disaster. A simple solution to these problems is to empower the ordinary citizen with their own means of measuring radiation levels. This thesis proposes the design of one such device, the Data Logging Radiation Detector.

2.1 Dangers of Nuclear Power

The production of electricity through nuclear processes accounts for a significant proportion of the world's energy demand. By the end of 2006, nuclear power generated about 15% of the world's energy [1]. According to the International Atomic Energy Agency (IAEA), at the end of that same year, there were 435 operational nuclear plants in countries throughout the globe. This makes nuclear power crucial to the global economy and livihoods of many millions of people. The significance of nuclear power cannot be downplayed, yet the risks surrounding nuclear power cannot be downplayed either.

Nuclear radiation is harmful to human health and evironment. Specifically problematic is that nuclear radiation is invisible, inaudible, odorless, and non-tactile; no human sense can detect it. For this reason it is necessary to use Geiger counters or other radiation detection devices to monitor radiation levels. This section will describe some of the inherent dangers of nuclear power production in attempt to highlight the need for ordinary citizens to have their own radiation measurement devices.

2.1.1 Aging Nuclear Plants

Aging nuclear power plants pose a significant threat to the safety of nuclear energy production. As of 2008, the average age of nuclear power plants across the globe was 24 years [2]. This number has been rising steadily for a number of years. Given the recent Fukushima disaster, calls for further nuclear investments have been quieted and the average age of nuclear plants is likely to continue to increase. In the United States, 48 of 104 plants have received 20 year renewal permits after their initial 40 year commissioning, meaning they will be over 60 years old when they are decommissioned. This trend is similar throughout the rest of the world.

As these plants get older, wear and tear of cooling systems, structure, and other essential components is inevitable. If these systems are not properly maintained, the likelihood of failure increases as the plants age. According to a bulletin by the IAEA [3], "if degradation of key components or structures is not detected before loss of functional capability, and if timely corrective action is not taken", then aging will directly affect the safety of nuclear power generation. Given the effect of aging on safety and the fact that ground was broken on all nuclear power plants in the United States before 1974 [4], aging is a significant issue in current and future nuclear energy discussions.

Even after the plants cease to produce power, they must be carefully decommissioned. Many of the radioactive materials within the nuclear reactors have half lives of thousands of years, meaning signifcant amounts will be present for a long time to come. Care must be taken in the handling of these materials and suitable locations must be found for their longterm safe keeping. These actions are in some ways more dangerous than normal plant operation because the processes are more complicated and rarely performed. Plus, transport and movement of radioactive materials is particularly risky.

2.1.2 Proximity to Population

In countries such as the United States and China, these nuclear plants are often located in areas with significant population densities. According to the journal *Nature*, 17.34 million people live within 75 km of the Indian Point nuclear plant in New York State. This number is relatively small compared to the 27.82 million within 75 km of Chinas Guangdong nuclear plant [5]. In total "one hundred and fifty-two nuclear power plants have more than 1 million people living within 75 kilometres" [5]. Special attention must be payed to these nuclear power plants as they pose risks to the large populations that surround them.

In the Fukushima nuclear disaster of March 2011, significant levels of radiation were found 80 km away from the plant [6]. The majority of the particularly harmful radioactive materials such as strontium-90 and americium-241 were not released because the concrete structure containing the reactor was largely left in tact [6]. If the concrete was destroyed by explosion such as in the Chernobyl disater of 1986, the contaminates would likely have traveled even greater distances, potentially reaching the population centers of Koriyama or Iwaka. The fukushima plant was relatively fortunate to be located far enough away from major populations. Even in cases such as Fukushima, when a plant is located far from people that means it is often located near argricultural areas which can be just as dangerous.

2.1.3 Unforeseen Threats

Even when redunancies and careful maintence are put in place in a nuclear power plants, some events cannot be prevented and can be just as—if not more—damaging than component failure or human error. Nuclear plants for the most part do not have built-in safegaurd for things such as natural disasters or terrorist attacks. These threats are known as "beyond design basis," meaning that nuclear plants are not designed to with these factors in mind [5].

2.1.3.1 Natural Disaster

Japan, even in with its high seismic activity, considered Fukushima to be a relatively low risk area for earthquakes and tsunami [5]. The engineering safeguards typically built into a nuclear power plant located near highly active seismic region were not completely implemented in the Fukushima case. Any damage caused by such an unforeseen event is likely to cause more damge as there are less safeguards and contingency planning is less thorough.

2.1.3.2 Terrorist Attack

Terrorist attacks are particularly threatening, albeit, more preventable and thereby less likely. A terrorist attack, however, would likely involve an explosive device putting a greater area and more people at risk. Considerable attention must therefore be paid to security measures around nuclear plants. Also, this threat can be accounted for after the plant is constructed as the threat does not pertain to any engineering regulations but rather the security surrounding the plant.

2.2 Demand for Geiger Counters

After the destruction caused by the tsunami and resulting nuclear power plant failure, many people—both in Japan and globally—flocked to purchase Geiger counters. Before the disaster, most people saw no need for measuring radiation themselves—at least now after the fact. Largely this was seen as a job for governmental and nuclear agencies. However, the events of March 2011 highlighted the fact that many people have a desire to measure radiation themselves. According to [8], many retailer sellers of Geiger counters such as Jim Flanegin's geigercounters.com had to shut down due to large demand in the days after the Japanese tsunami. For a period of weeks to months after, virtually all Geiger counters were out of stock across all internet retailers.

The demand for Geiger counters was so high in the period directly after the Fukushima disaster that counterfit Geiger counters were a serious problem. According to one report [9], Geiger counters had "sold out and prices quadrupled in Tokyo because of worries about radiation fallout since the Fukushima nuclear reactor meltdown...The demand spurred a grey market of 'illegal' products that use faulty parts and shoddy designs or are fake." Unfortunately, some companies apparently took advantage of the fear and desperation that many Japanese were feeling after the tragedy. With a new awareness of the importance of radiation detection, consumers can be better prepared and obtain a Geiger counter before the next nuclear disaster hits.

2.3 Governmental Response to the Fukushima Disaster

Unfortunately, the threat of nuclear disaster can hardly be considered a "potential" given the large-scale damage caused by previous nuclear power plant failures. According to an article in the journal *Nature*, 1.73 million people lived within 75 km of the Fukushima Daiichi plant when its three reactors failed and cores melted after a tsunami in March 2011 [5]. The disaster was rated a seven out of seven on the international nuclear events scale [7]. The amount of radiation released, 7.7×10^{17} Becquerel, is the second largest amount ever, only surpassed by the Chernobyl explosion in 1986 [6]. The damage caused by the Fukushima disaster was been widely chronicled by media outlets.

The desire to measure radiation oneself can be due to many factors. Chief among the concerns after the Japanese disaster was the reliability of governmental data. Given that radiation sickness can be potentially lethal, the threat of radiation is a significant one. If governmental numbers are off for some reason, the damage could be irreversible. This concern of governmental data is not unfounded. According to a report by a Japanese government panel, "From inspectors' abandoning of the Fukushima Daiichi nuclear power plant...to a delay in disclosing radiation leaks, Japan's response to the

nuclear accident caused by the March tsunami fell tragically short" [10]. The Japanese government's handling of the Fukushima disaster did not inspire confidence in their abaility to handle the situation effectively and therefore citizens were unsure whether or not the government's data could be trusted.

A second concern after inaccurate data is having no data at all. If the nuclear fallout is great enough, it may prevent governmental agencies from gathering data. Another potential issue could be that the power is out and a person has no means of communication. Under any type of disaster scenario, the average citizen is scared for their health, unprepared, and will attempt to seek safety. In the case of a nuclear disaster, having a Geiger counter enables the user to determine first hand and with confidence, whether or not their familys, friends, or own life is at risk. A Geiger counter can empower its user, providing them with a sense of security and making them safer.

2.4 Radiation Measurement

Radiation can be confusing to the layperson. The typical person only has an understanding of radiation from news, movies, or books. Largely these sources tend to sensationalize radiation, focusing on the danger of nuclear fallout and ultimately leaving people scared or confused.

There are two types of radiation: non-ionizing and ionizing. An example of non-ionizing radiation is the RF signals produced by mobile phones or microwaves. These sources are non-ionizing meaning that they do not break chemical bonds. They are therefore considered less harmful. In high enough power densities these sources will cause heating but they are not believed to cause cancer. Ionizing radiation is more harmful to human health as it can potentially break chemical bonds and cause cellular damage, thereby causing radiation sickness or cancer [11]. Geiger counters are capable of measuring only ionizing radiation. Ionizing radiation comes from both natural and man-made sources. Figure 2.1 below shows the percent that each type of source

contributes to the total radiation contamination each person receives. From the figure
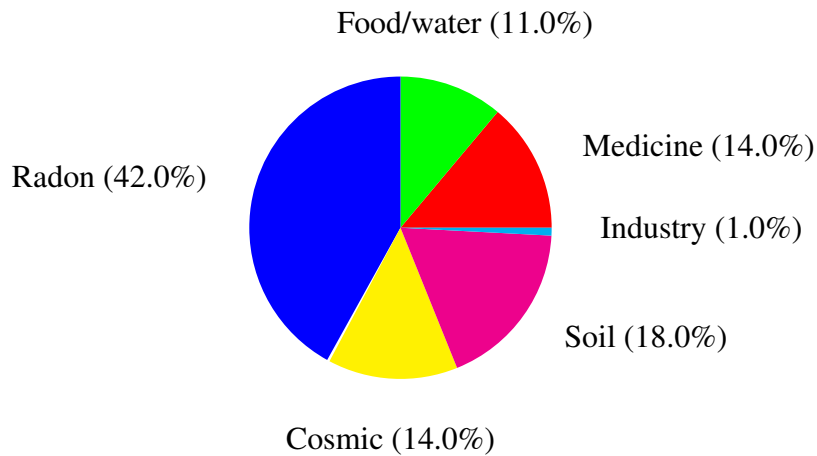
Figure 2.1. Radiation sources and relative percentages [12]

one can see that natural radiation accounts for 85% of the total radiation received each year while the nuclear power industry accounts for only 1%.

There are two measures of ionizing radiation. First is the radiation concentration. Radiation concentration can be broken down into two measures: dose, and counts per minute (CPM). The dose can be thought of as a relative concentration of radioactive particles within an object or person. The radiation dose is measured in SI units of grays (Gy). CPM is a measure of the number of nuclear decays that occur in one minute. This is the measure that Geiger counters will detect: for each radioactive particle that strikes the Geiger tube, a detection is recorded and the operator is typically alerted by a clicking noise from the device. The second measure of radiation has to do with the human harmfulness the radiation. The type of radioactive particle emitted and the concentration of radioactive particles dictate the harmfulness. As mentioned before there are three types of ionizing radiation: alpha particles, beta particles, and gamma rays. In terms of human health, the alpha particle is the most dangerous while the beta particle and gamma ray are less dangerous. (Alpha particles are more harmful to human tissue than the other two forms of ionizing radiation but they are also the most easily shielded and can be stopped by a piece of paper. They are therefore only dangerous if ingested or

9

emitted inside the body [12]. Beta particles can penetrate slightly into human tissue and gamma rays an penetrate significantly further than beta particles.) The measure of this harmfulness is called relative biological effectiveness (RBE) and is measured in SI units of sieverts (Sv) [13]. In order to measure RBE, the type of ionizing radiation as well as the concentration of the radiation must be taken into account, making this a more difficult measurement to carry out. This is because it is more difficult to discern between types of ionizing radiation than it is to simply detect one of the three types of ionizing radiation. Once the type of radiation is determined, the relative concentrations of each type must be determined and then a calculation must be performed to achieve the final RBE measurement in sieverts. From Figure 2.1, if one assumes a total radiation level of 2.4 mSv/yr as suggested by [12], industry accounts for only 24 μSv/yr. In the case of the Fukushima disaster, however, within an 80 km radius, radiation levels were over 6,000 times greater than background. In a disaster such as Fukushima, nuclear industry would account for $> 99\%$ of radiation totaling in at upwards of 10,000 mSv/yr.

For most applications, especially consumer devices, measurements of RBE become prohibitively expensive and therefore impractical. Moreover, to determine the dangerousness of radiation levels, RBE measurements are unnecessary. In most cases, measurements in CPM are adequate in alerting the user of potential harm. For instance, typical background radiation levels are 15–25 CPM. Anything in the range of 100–10,000 can therefore be considered significant radiation levels and anything greater than 10,000 is extremely unsafe. In the case of a consumer level Geiger counter, the user is not concerned with scientific level accuracy in their measurements but is more concerned with relative safety. That is, if they measure 1,000 CPM around their milk or water, they should be suspicious of the source and proceed accordingly.

2.5 Proposing a Device Design

This section compares a commercially available Geiger counter to an ideal Geiger counter that would be able to suit mass market demand and provide reliable and valuable data in time of distress such as the Fukushima disaster.

2.5.1 Existing Design

Since the Japanese nuclear disaster, many companies have begun to produce and sell Gegier counters for hobbyists. One such device is a Geiger counter by Sparkfun Electronics[1]. This device sells for $149.95, making it relatively inexpensive compared to other products. In the Sparkfun Geiger counter, data is sent serially to the user's PC. This means the Geiger counter must be connected to a computer at all times in order to transmit data. The Sparkfun Geiger counter runs into many of the same problems that other Geiger counters face—in order to measure radiation, the user must be close to a source of radiation. This is acceptable when radiation levels are low enough to be harmless; however, high levels of radiation are harmful to human health. For any portable application, the device must be permanently connected to a power source, namely a PC. This makes such a device impractical and potentially dangerous.

2.5.2 Improved Design

The ideal consumer device would allow for realtime remote data output or "after-the-fact" storage and retrieval of data. While realtime output is generally convenient, wireless transmission of data requires significantly more power than an SD card, meaning shorter battery life. Thus, for a portable design SD card is ideal. The SD card can store the data and the device can be retrieved when or where radiation levels are safe for humans. Once the device is retrieved, the data from the SD card can be read and plotted

---

[1] http://www.sparkfun.com/products/10742

with a personal computer. Since the device is small (approximately 6 in. $\times$ 2 in.) it can be put on a robot, balloon, or any other autonomous vehicle.

Other than removable memory, the Geiger counter should be affordable and easy to use. These factors are the most critical if widespread adoption is desired. Device design of the Data Logging Radiation Detector addresses these issues in the remaining chapters.

Chapter 3

PROJECT BREAKDOWN

This chapter provides a general overview of device deisgn and layout, particularly focusing on how the project blocks work together to form a cohesive device capable of reliably measuring radiation.

3.1 Specifications

Specifications were chosen in order to ensure the reliability of the Data Logging Radiation Detector. Table 3.1 indicates these project specifications. The specifications are important as they form a baseline level of performance that must be achieved in order for the radiation detector to operate correctly.

Each specification serves a particular purpose. Output voltage is important as it dictates whether or not the Geiger tube is operational. Efficiency is important as it is directly proportional to battery life. Finally, accuracy is important as incorrect measurements can be misleading to the operator and potentially harmful to human health. By

Table 3.1. Project specifications

Specifications	Proposal
Output voltage	495–605 V
Power supply efficiency	60%
Count per minute accuracy	85%

meeting the specifications of the project proposal, located in Appendix A and duplicated above in Table 3.1, it is possible to ensure that the Data Logging Radiation Detector is functional, accurate, and does not waste power, making it suitable for all users in a disaster zone.

3.2 Project Blocks

The project is broken down into four major blocks: boost switching power supply, Geiger tube, microcontroller, and SD card. Figure 3.1 shows each block's relation to one another and to the project as a whole. The inputs to the project are a 5 V DC source at the boost switching power supply and alpha, beta, or gamma radiation at the Geiger tube. The outputs of the project are a text file written to an SD card and a digital signal from a microcontroller that illuminates a light emitting diode (LED).

```
┌──────────────┐      ┌──────────────┐      ╭──────────────╮
│    Boost     │      │              │      │    Alpha,    │
│   Switched   │ ───► │ Geiger Tube  │ ◄─── │   beta, or   │
│ Mode Power   │      │              │      │    gamma     │
│   Supply     │      │              │      │  radiation   │
└──────────────┘      └──────┬───────┘      ╰──────────────╯
                             │
                             ▼
                      ┌──────────────┐      ┌──────────────┐
                      │ Microcontroller│ ──► │   SD Card    │
                      └──────────────┘      └──────────────┘
```
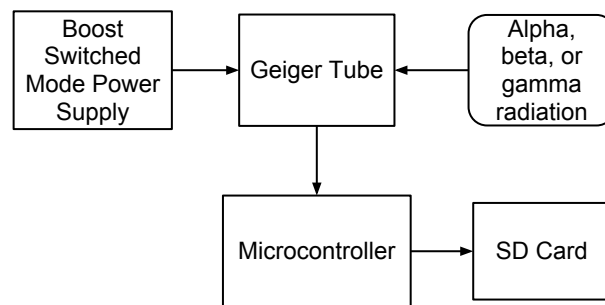
Figure 3.1. Block diagram illustrating the major components of the project

The following sections will describe how each block interacts with the other blocks to produce the desired outputs of data in units of CPM stored to an SD card and a digital signal to indicate the detection of radiation (illuminating an LED). Specifically, Section 3.2.1 describes the Geiger tube's operation. Section 3.2.2 describes the switching power supply. Finally, Sections 3.2.3 and 3.2.4 describe the microcontroller and SD card, respectively.

3.2.1 Geiger Tube

While the boost power supply is the first block of the project as seen in Figure 3.1, the boost power supply's characteristics are governed by what it is powering—the Geiger tube. It is therefore beneficial to explain the Geiger tube's operation first. This discussion will make the need for the power supply obvious and will help determine

the design requirements for the boost power supply. It is also relevant to explain the operation of the Geiger tube first since it is what converts radiation into an electrical signal and therefore is the most important single component of the project.

Figure 3.2 shows the physical structure of the Geiger tube. The Geiger tube itself
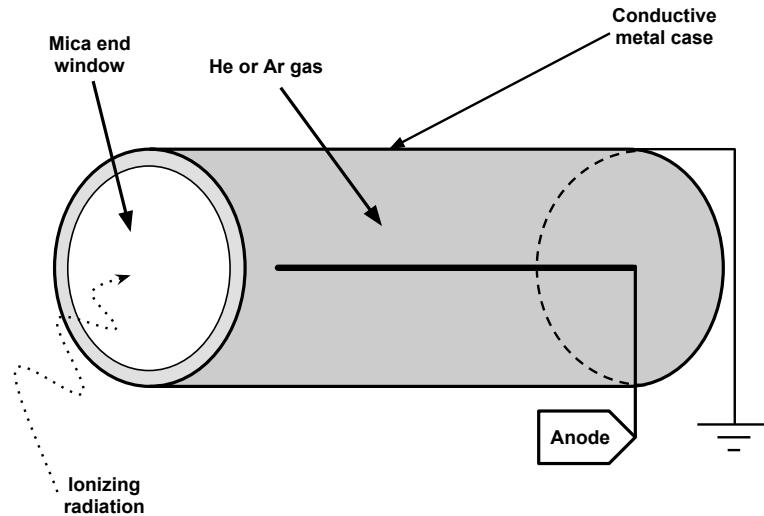
Figure 3.2. Geiger tube schematic drawing

consists of a metal tube filled with either helium or argon gas. The anode of the tube is placed in the center, surrounded by the gas. The cathode is electrically connected to the outer shell of the tube. A high potential ($\approx$ 550 V) is placed across the anode and cathode. When a radioactive particle/wave collides with and enters the tube, the high voltage will cause the radiation to ionize the gas molecules. Electrons are then ejected from the gas atoms. The negatively charged electrons are attracted to the positively charged anode [15]. This flow of electrons results in a pulse of current at the cathode of the tube.

A microcontroller can be set to interrupt when the pin connected to the tube anode goes high. This forms the basic process for the detection of a radioactive particle/wave.

3.2.2 Switching Power Supply

In order to properly bias the Geiger tube, a voltage on the order of 500 V must be placed across the anode and cathode of the tube. Such a high voltage is not directly available from batteries, lab power supplies, or wall outlets. To generate this voltage, a boost DC-DC switching power supply is necessary. According to the specifications of Table 3.1, the boost power supply must have an output voltage from 495–595 V and an efficiency of greater than or equal to 60%. Usually such a high voltage would imply high power consumption. This is not true for this particular application. Since the impedance of the tube is nearly infinite (only significant when the tube is transmitting a pulse of current), the output current is very low and therefore output power is very low. The total power consumed by the power supply is small enough that the device can run off batteries.

3.2.3 Microcontroller

The microcontroller performs multiple functions for the device. These functions can be broken into two main types: analog (power supply related) tasks and digital (SD card and LED) tasks.

3.2.3.1 Analog Tasks

The microcontroller regulates the boost switching power supply. The microcontroller does this by reading a voltage from a resistor divider at the output of the power supply. Based on the voltage read by the analog to digital converter (ADC), the microcontroller generates a pulse width modulated (PWM) square wave that then drives the switching MOSFET. This process is described in greater detail in Section 4.

3.2.3.2 Digital Taks

The microcontroller performs a series of digital tasks simultaneously. First, the microcontroller detects and stores CPM data that is input via the Geiger tube. The microcontroller does this by enabling an interrupt service routine (ISR). When the ISR pin on the microcontroller is triggered by a falling edge, the ISR stops any running processes and enters into the routine. In the routine, the microcontroller is programmed to receive the data and save each count to internal memory.

The next task that the microcontroller performs is the illumination of an LED. After data has been received and stored by the microcontroller, a digital pin is driven high by the microcontroller. A series resistor is attached to this pin, limiting the current through the LED. Each time the LED lights up, a particle has been detected. The illumination of the LED provides a visual cue to the user, ensuring them that the device is functional. This is beneficial as the user is unable to see internal processes at play and hence making it difficult to troubleshoot any potential problems.

Next, the microcontroller writes the CPM data to the SD card every minute. Once the device is programmed and powered, an internal timer inside the microcontroller will run for one minute. Each count is accumulated in internal register over this one minute interval. Once the minute is up, the total number of counts in the one minute period is written as a text file to the SD card.

The final task that the microcontroller performs is the illumination of a second LED, used to alert the user that an error occurred in writing to the SD card. If the SD card is not recognized by the microcontroller, a red error light will appear indicating the need for insertion (or reinsertion) of the SD card.

3.2.4 SD Card

The SD card is the data storage component of the Data Logging Radiation Detector. An SD card is the ideal storage for the device for multiple reasons. First, SD cards

are very inexpensive. A 2 GB SD card runs from $3-6. Second, SD cards are widely used. They are the standard storage device of digital cameras and can be found in many other devices such as cell phones and MP3 players. All major operating systems and computers thereby support the SD card standard. Third, SD cards are non-volatile, meaning they retain their stored data even when powered off. Non-volatility is necessary if the device runs out of power—a potential senario for any portable device. Fourth, SD cards consume very little power. Low power means better battery life. Finally, SD communication is relatively simple when compared to USB communication.

Chapter 4

DESIGN

The following section delves into the details of how each block operates. Subsection 4.1 focuses on the switching power supply, Subsection 3.2 focuses on the microcontroller, and Subsection 3.3 focuses on the SD card.

4.1 Switching Power Supply

Multiple considerations were taken into account when designing the switching power supply. The most important parameters were the input voltage and current and the output voltage and current.

4.1.1 Input Power

For the input voltage, 5 V DC was chosen. The project proposal allowed for any DC voltage in the range of 3–12 V. Five volts was deemed the optimal voltage as it was known that the microcontroller was likely to run off a 5 V source. Using a 5 V input to the power supply means the power supply and microcontroller blocks could share the same input voltage source, simplifying the required circuitry. The selected 5 V is also the standard voltage for USB communication. Since 5 V is the only input voltage, the programmer is able to not only program the microcontroller, but also power the entire Data Logging Radiation Detector.

The second factor in determining the input power is input current. The input current is determined by the switching power supply. By designing the power supply properly, input current was minimized. The input current is dictated by duty cycle of the square wave driving the switching MOSFET, inductor size, and other factors. The analysis in 4.1.5 will describe how these values were chosen to find a suitable balance between input current and output voltage.

4.1.2 Output Power

The output voltage and current requirements were dictated by the Geiger tube. The tube selected for this device was the LND712 from LND Inc. This tube is used in many other inexpensive Geiger counters, including the Sparkfun Geiger counter. The tube requires a median voltage of 550 V, so this voltage was chosen as the median operating voltage in the Project Proposal (see Appendix A). At DC with no radiation, the impedance seen looking into the Geiger tube is nearly infinite. (The only current output from the tube is associated with the capacitance of the tube. In other words, only upon the detection of a radioactive particle will a current be discharged and the impedance appear finite.) An infinite impedance means no output current hence no output power and an efficiency of 0%. Since power supply efficiency needs to be greater than or equal to 60% according to Table 3.1, an output load resistance, R_{out}, was placed from V_o to ground. This allows for a continuous current to flow through R_{out} and therefore establishes an output current and a positive power supply efficiency. The selection of R_{out} is described in 4.1.7.

4.1.3 Boost Switching Power Supply Operation

A boost DC–DC switching power supply converts a lower voltage DC input voltage, V_i, to a higher DC output voltage V_o. In this design $V_i = 5$ V and $V_o = 550$ V. The basic topology of a boost switching power supply can be seen below in Figure 4.1. The circuit is called a switching power supply because the switch controls the state of operation (in practical implementations, this switch is a transistor).

At some time, say, $t = 0$, the switch is open. Inductor L_1 appears as a short under DC conditions and dumps any stored energy in its magnetic field to C_o. Meanwhile V_i appears at the diode's anode, therefore making D_1 forward biased. Current is conducting through D_1 and charge is stored onto the output capacitor, C_o. This charge build-up on C_o creates some output voltage (less than the desired V_o). This state where the switch is
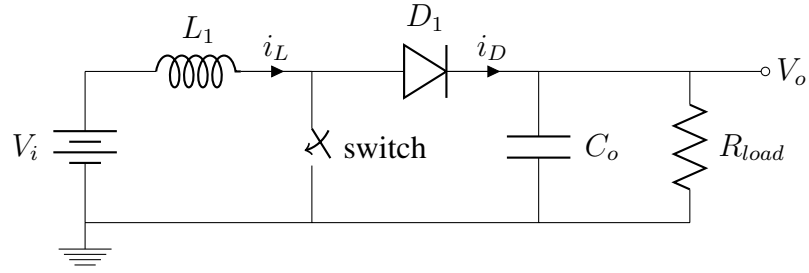
Figure 4.1. Boost DC-DC switching power supply topology

open is the "off" state of the boost switching power supply. The total time in this state is called T_{off}.

At time $t = t_2 = T_{off} + T_{on}$, the switch is closed. The inductor sees an instantaneous change in voltage across its terminals (from 0 V to 5 V) so current ramps up linearly in the inductor [16]. This state where the switch is closed is the "on" state of the boost switching power supply. The total time in this state is called T_{on}.

The ratio of T_{on} to the total period $T \times 100\%$ is the duty cycle. Selecting a larger duty cycle means that a higher output voltage is possible. On the other hand, larger duty cycle means greater input power and therefore greater input current and likely lower efficiency. It is necessary to balance output voltage with efficiency such that each meets the required specifications.

By rapidly switching between the "on" and "off" states, charge on C_o gradually builds until the output voltage V_o is reached. This voltage is regulated in a negative feedback loop with the microcontroller. The particular feedback control scheme implemented by the microcontroller is described in 4.2.4.

4.1.4 CCM vs. DCM

The boost switching power supply can operate in two distinctly different modes, continuous conduction mode (CCM) and discontinuous conduction mode (DCM). CCM occurs when the inductor current i_L does not reach zero, whereas in DCM i_L does reach

21

zero. Each mode functions very differently and is appropriate for different applications. According to [17], for low load currents it is desirable to operate in DCM. DCM has the benefit of being able to produce higher output voltages with smaller inductor sizes but has the downside of producing higher peak currents which can result in AC switching noise on DC power lines [17]. The output current of the Data Logging Radiation Detector is approximately $550 \text{ V}/R_{out}$. For an arbitrary output resistance of 1 MΩ the output current is approximately 500 μA. This is low for a typical power supply and thus it is appropriate to select DCM as the operating mode. Section 4.1.5 will describe the selection of components assuming operation in DCM.

4.1.5 Power Supply Component Selection

In the ideal analysis of a boost switching power supply in DCM, the output voltage is a function of input voltage, V_i; inductor size, L_1; switching frequency, f; duty cycle, $d = \frac{T_{on}}{T} \times 100\%$; and output resistance, R_{out}. From [16], the relationship between input and output voltages is given as

$$V_o = V_i \sqrt{\frac{k R_{out} \frac{d}{1/f}}{2 L_1}} \tag{4.1}$$

where k represents some fraction of the total period. In the case of this design, some values are have been predetermined. These are: $V_i = 5$ V, $V_o = 550$ V, and $f = 4$ kHz. This analysis also assumes that $k = 1$, meaning that $T_{on} + T_{off} = T$, or that the inductor current reaches zero exactly at the end of one cycle. The frequency is known to be 4 kHz because the microprocessor can only generate a PWM signal at certain frequencies, as will be seen later.

Using Equation (4.1), it is possible to establish preliminary component values. Solving Equation (4.1) for L_1 and assuming $R_{out} = 1$ MΩ and a 50% duty cycle results

in

$$550 \text{ V} = 5 \text{ V} \sqrt{\frac{1 \text{ M}\Omega \times 125 \text{ } \mu s}{2L_1}} \Rightarrow L_1 = 5 \text{ mH} \tag{4.2}$$

These values were then experimentally tested to check that the output voltage and efficiency specifications were met. From these tests it was found that values of $L_1 = 10 \text{ mH}$, a duty cycle near 60%, and output resistance of $R_{out} \approx 5 \text{ M}\Omega$ gave the appropriate output voltage. R_{out} was adjusted as described in the following subsection to make sure that the efficiency met specification. The selection of the duty cycle is also described in 3.2.

Since the output voltage was expected to be 550 V, high voltage components needed to be used. Specifically, the drain to source voltage (V_{DS}) of the switching MOSFET and the breakdown voltage of the diode (V_{bd}) needed to be greater than 550 V. After these necessary requirements were met, the efficiency of each component was taken into account. Specifically, the equivalent series resistance, R_{DS}, was minimized when selecting a MOSFET. Higher R_{DS} causes heat to accumulate in the MOSFET, increasing switching losses and potentially decreasing the MOSFET's lifetime. The inductor's series resistance R_L also decreases efficiency. For these reasons, an inductor with low R_L was selected.

4.1.6 Geiger Tube Impedance

As mentioned before, the input impedance seen looking into the Geiger tube is infinite at DC, assuming no particles are being detected. The capacitance associated with the tube is discharged every time a particle is detected. This capacitance is related to the avalanche of electrons that are ejected from the helium gas molecules inside the tube. If a 5 pF tube capacitance is assumed (relative estimation based on the dimensions of the tube) it is possible to solve for the energy discharged per detection

$$E = \frac{1}{2}CV^2 = \frac{1}{2}(5 \text{ pF})(550 \text{ V})^2 \approx 0.75 \text{ } \mu J \tag{4.3}$$

23

Therefore there is an associated discharge of 0.75 μJ of energy with each detection. If 20 CPM is assumed (standard background radiation level) one can solve for the average current at the output of the Geiger tube

$$i(t) = C\frac{\mathrm{d}v(t)}{\mathrm{d}t} \Rightarrow i = 5 \text{ pF}\left(\frac{550}{3}\right) \approx 1 \text{ nA} \qquad (4.4)$$

Where $\mathrm{d}t = 3$, the average time between detections in units of seconds. The resulting current leaving the tube, 1 nA, is negligible considering with a load resistance of 5 MΩ, the load current is 110 μA. This means the average CPM would need to be five orders of magnitude larger in order the tube output current to be roughly equal to the load current. In other words, even with a high CPM rate on the order of 1000 CPM, the switching power supply would be able to deliver the required voltage to power the tube. This analysis does rely on the assumption of a 5 pF capacitance associated with the tube. However, even a 5 nF capacitance would not affect the output voltage significantly following the above analysis.

The above assumed a 5 MΩ shunt resistance. The reason for this is simple: Since this associated output current is so small, 60% efficiency is nearly impossible to acheive without a DC path to ground. For this reason, a shunt resistance was added at the output of the power supply. This allows a DC current to flow from the output of the switching power supply to ground, improving overall efficiency but increasing total consumed power. Ideally this would not be necessary, however, project specifications must be meet according to how they are written in Appendix A.

4.1.7 Output Resistance and Resistor Feedback

Figure 4.2 shows how the selected output resistance affects the overall power supply efficiency. When the resistance is small such that $R_{out} = 0 \ \Omega$, there is no voltage at the output so the expected efficiency is 0%. As the load resistance gets very large such that $R_{out} = \infty$, (as with the Geiger tube) the output current approaches 0 A.
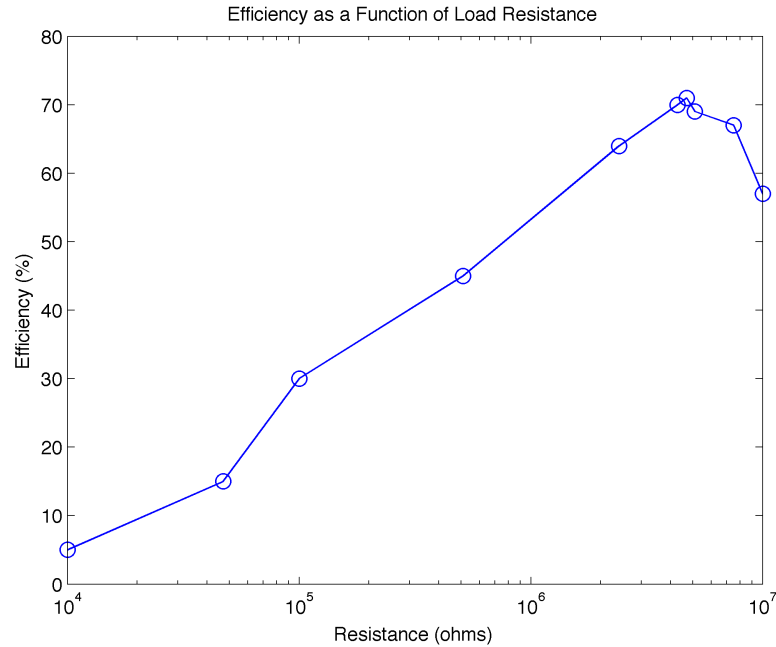
Figure 4.2. Power supply efficiency as a function of load resistance—experimental results plotted with logarithmic x–axis

Zero output current also corresponds to an efficiency of 0%. Figure 4.2 confirms this. Experimentally it was found that the resistance that gave the highest efficiency was 4.7 MΩ. For this reason, R_{out} was selected to be 4.7 MΩ.

The total output resistance needed to be close to 4.7 MΩ; however, a second resistor was needed to establish a feedback path to the microcontroller. Since most microcontrollers' ADCs can read a maximum of 5 V—not the 550 V at V_o—a resistor divider was established at the output. The resistor divider ensures that the majority of the voltage drop occurs across the 4.7 MΩ resistor and thereby provides a voltage from 0–5 V, which is the operable range for the ADC. It is thereby possible to get a voltage proportional to the actual output voltage—only scaled down such that this voltage would not damage the microcontroller. Figure 4.3 shows the feedback resistor divider setup.

R_1 was selected such that when $V_o = 550$ V, the voltage seen at V_{ADC} would be 2 V since 2 V is 40% of 5 V. The resistor values are small compared to the 100 MΩ
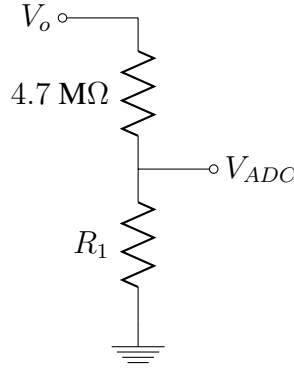
Figure 4.3. Feedback resistor setup

input impedance of the ATMega 328p, therefore it can be reasonably neglected from the analysis. Negative feedback was utilized for the power supply; therefore, 40% becomes 60% when the bits are complemented. Therefore, a duty cycle of approximately 60% is required for an output voltage in the 500 V range. Any voltage increase at the output would also increase V_{ADC} but not by enough to make $V_{ADC} > 5$ V. Using these conditions to solve for R_1 one has

$$550 \text{ V} \left(\frac{R_1}{R_1 + 4.7 \text{ M}\Omega} \right) = 2 \text{ V} \Rightarrow R_1 \approx 21 \text{ k}\Omega \tag{4.5}$$

With this value for R_1, an output voltage of $V_o = 1124$ V would be necessary to damage the microcontroller. Even with 100% duty cycle driving the MOSFET, it would be virtually impossible to exceed this voltage and damage the microcontroller. The total output resistance essentially remains the same since 4.7 MΩ + 21 k$\Omega \approx$ 4.7 MΩ. The total power supply efficiency also remains the same.

4.2 Microcontroller

The microcontroller serves many critical purposes in this project. It controls all digital functions for the device and integrates the various blocks into a unified device that performs the desired functionality. The microcontroller controls the power supply

26

by analyzing feedback from the output and adjusting the duty cycle of the power supply, thereby controlling the output voltage. The microcontroller also senses the signal from the Geiger tube, converts the detection into a digital output, and accumulates the CPM data over the one minute period. Finally, the microcontroller communicates with the SD card and saves the CPM data in a comma separated value (CSV) format.

For the above reasons, selecting an appropriate microcontroller was critical to device performance. The microcontroller must be capable of performing these multiple tasks as well as potential improvements.

4.2.1 Selection of Microcontroller

The selection of a microcontroller for this project was made based on several considerations including:

- Price

- Availibility

- Ability to perform PWM at or near 4 kHz

- Analog to digital converter

- Multiple timers

- SPI interface to communicate with a SD card

After careful consideration of the above constraints, an Atmel ATmega328p microcontroller was selected. Research indicated the 32 KB of internal flash memory would be sufficient to utilize existing libraries necessary for SD card communication. The ATmega328p would be capable of PWM at approximately 4 kHz, and the 16-bit timer 1 could time one minute periods, both while operating with the internal 1 MHz clock.

It has 6 A/D converters, and excess I/O pins that allow for flexibility with future modifications. Overall, the ATmega328p meets all the technical constraints of the project. In addition, it is inexpensive at $5.

4.2.2 Power Supply Control

The microcontroller controls the power supply output voltage through a series of sequential steps. First, the ADC reads an analog voltage seen between the output resistor divider. Next, based on the voltage read by the ADC, a 4 kHz PWM signal drives the gate of the switching MOSFET. If a low voltage is read, the microcontroller compensates by generating a PWM signal with a high duty cycle. This boosts the output voltage by supplying more current to the boost stage. If the read output voltage is too high, the microcontroller generates a lower duty cycle PWM signal, causing the opposite effect.

Since the output voltage is on the order of 500 V, a simple voltage divider was attached to the output in order to bring the voltage seen at the pin of the microcontroller down to within the range of 0–5 V. This was done to prevent a high voltage from damaging the microcontroller. The selected values for the resistor divider can be seen in Figure 4.3.

4.2.3 Analog to Digital Converter

The microcontroller reads a voltage from zero to five volts at the resistor divider. The ADC converts this to a digital value from 0–255. The ADC is used in single conversion mode, where the conversion is performed on demand. To make the process of selecting the appropriate ADC and reading the resulting output more intuitive, a function, `adc_read()`, was written that takes the ADC number as an input and returns the converted result. [This function was written by Brian.] As a high degree of accuracy is not necessary for this application, 8-bit precision for the analog to digital conversion

was selected. Source supply voltage, V_{cc}, was selected as the reference voltage. Since the ADC must be clocked at a frequency between 50 and 200 kHz, a clock prescaler of 8 was selected based on the 1 MHz clock. The application of these settings can be seen in the code for the function `adc_read()` starting at line 148 of the project code in Appendix C.

4.2.4 Pulse Width Modulation

To change the output voltage based on the voltage read by the ADC, the duty cycle of the signal driving the MOSFET gate must be altered. The signal driving the MOSFET is pulse width modified, meaning that the frequency of the signal stays the same, but high time and low time of the signal are altered inversely. The microcontroller generates the PWM signal using `timer0` set to non-inverting fast PWM mode. The clock divider set to 1 produces a signal at about 4 kHz when using the internal 1 MHz clock. The `OCR0A` register controls the duty cycle of the signal, which is set to the complement of the return value from `adc_read()`, providing negative feedback. [Brian implemented this with the general principle established by the two of us.] Taking the complement of the return value is equivalent to $255 - ADC\_value$ since the values are unsigned. With the above settings, a 60% duty cycle results in an output voltage of approximately 500 V. The feedback voltage divider was altered slightly so that the voltage that appears at the microcontroller is approximately 40% of 5 V, or 2 V.

The application of the PWM signal settings can be seen in the code for the function `pwm_init()` starting on line 123 of Appendix C and the application of the feedback controlling the duty cycle can be seen on line 80 of Appendix C.

4.2.5 Geiger Tube Signal Sensing and Digital Output

The signal being fed to the microcontroller from the Geiger tube is a signal that is normally high and drops sharply upon detection of a particle as shown in Figure 4.4.

To sense this drop, an external interrupt pin is utilized and set to interrupt on falling edge
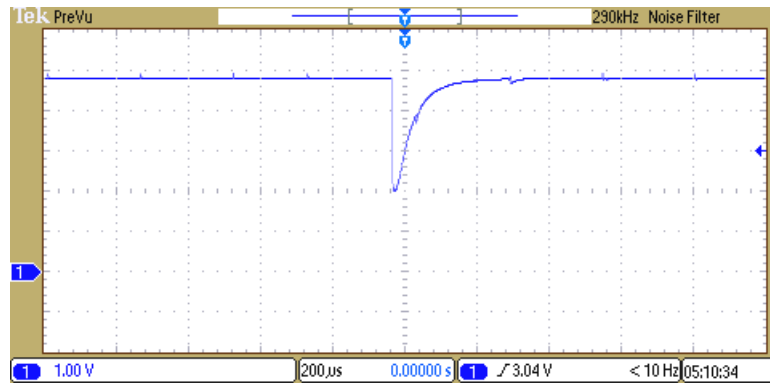
Figure 4.4. Oscilloscope waveform of geiger tube output

only. The ISR is very short, consisting only of setting a flag and incrementing a CPM variable. The interrupt is kept as short as possible so that if two detections occur very rapidly both will be counted. The code periodically looks at this flag and if set, lights a status LED (light emitting diode) for 100 ms to indicate the detection. The application of the Geiger tube signal sensing can be seen in various locations in the code. The most significant portions are on lines 81-86 and lines 110-130 of the project code in Appendix C. [Brian wrote the ISR.]

The other digital output of this project is the CPM data. The method for calculating CPM is simple: increment a variable with every detection, and timing out after one minute. When the minute expires, the CPM variable is saved and reset, then the timer begins the count for the next minute interval. The application of this method involves using `Timer1` in the ATmega328p to time one minute, and generate an interrupt when the timer expires. The contents of this interrupt service routine set a flag, which causes the above sequence of events to happen. `Timer1` is set up to "clear timer on compare", causing the interrupt upon a compare match. The value of the comparison is calculated as shown below:

$$\texttt{OCR1A} = \left(\frac{1 \text{ MHz Clock Speed}}{1024 \text{ Clock Dividor}} \times 60 \text{ sec} \right) - 1 = \texttt{0xE4E1} \tag{4.6}$$

30

The application of `Timer1` can be seen in lines 87–98 and lines 132–138 of the project code in Appendix C. The status LED allows for real-time monitoring of radiation levels, while the SD card allows for future data analysis.

4.3 SD Card

In implementing the addition of an SD card to the project, the decision was made to utilize existing libraries to handle the low-level serial peripheral interface (SPI) communication with the SD card. [Brian worked with these low-level libraries.] With the functions provided in these libraries, communicating with the SD card becomes similar to interfacing with files in C on a standard file system with standard C libraries. The microcontroller initializes the SD card and file system, creates a file and file pointer, and every minute writes the CPM count to file. An eject button informs the software that the user intends to eject the SD card, causing the file to be closed and an LED to illuminate, indicating the process has finished. The implementation of the SD card data logging can be seen in the project code of Appendix C.

Interfacing with the SD card, which operates at 3.3 V, involves using a voltage divider on the pins connecting to the ATmega328p. All of the signals coming from the microcontroller are dropped to 3.3 V through the voltage divider to ground, and all signals from the SD card at 3.3 V are sufficient voltage for the microcontroller to read. The resistor values were selected to be small relative to the approximately 75 kΩ input resistance of the SD card pins, 1.8 kΩ and 3.3 kΩ produce the necessary voltages. The SD card connects to the MOSI, MISO, SS, & SCK ports on the ATmega328p, which can be seen on the project schematic in Appendix B.

Chapter 5

RESULTS

The results section briefly describes the test methodology and rationale while focusing on test results. Subsection 5.1 describes how the output voltage was measured and describes the associated results. Subsection 5.2 explains efficiency testing methodology and results. The final subsection 5.3 describes the accuracy measurements and results.

5.1 Output Voltage

The first step of testing was to determine if the output voltage of the switching power supply met specifications. If the output voltage of the switching power supply is not high enough, the Geiger tube will not be able to operate.

To test the output voltage, the lab multimeters were used. These multimeters have a DC input resistance of 10 MΩ. Usually, when measuring a voltage across a resistor, the input resistance of the multimeter does not affect the actual quantity that is being measured. For example, if measuring 1 V across a 1 kΩ resistor with a 10 MΩ multimeter, the resistance of the multimeter acts in parallel with the 1 kΩ resistor, creating an equivalent resistance of

$$R_{eq} = \frac{R_1 \times R_2}{R_1 + R_2} = \frac{10 \text{ G}}{1 \text{ k} + 10 \text{ M}} = 999.9 \ \Omega \qquad (5.1)$$

which is essentially the same value as the 1 kΩ resistor. In other words, neglecting the effect of the measurement tool on the circuit results in a very small error.

If, however, one is measuring the voltage across a larger resistor, say the 4.7 MΩ output resistance of the power supply, the input resistance of the multimeter is not negligable. The equivalent resistance with the multimeter attached is

$$R_{eq} = \frac{47 \times 10^{12}}{14.7 \times 10^6} = 3.1973 \text{ M}\Omega \tag{5.2}$$

which is 32% less than the desired 4.7 MΩ resistance. The discrepancy means the reading on the multimeter would actually show the voltage across the 3.2 MΩ equivalent resistance, not the voltage across the 4.7 MΩ resistance that is at the output under normal operating conditions.

To compensate for the lower-than-desirable input resistance of the lab multimeter, 90 MΩ was put in series with the multimeter resulting in an equivalent resistance of 100 MΩ. The equivalent output resistance of the power supply with the multimeter attached is $R_{eq} = 4.489$ MΩ which is only 0.044% less than 4.7 MΩ. The added series resistance with the multimeter forms a 1/10 voltage divider, it is necessary to correct the measurement by simply multiplying the multimeter's reading by ten.

The voltage measured at the output of the power supply is 514 V, which is within the specified range of 495–595 V.

5.2 Efficiency

Efficiency of the power supply is calculated as

$$\text{Efficiency} = \frac{P_{out}}{P_{in}} \tag{5.3}$$

Measuring the efficiency of the power supply is more complicated than it may first appear. The problem lies in the fact that the microcontroller performs functions for the power supply as well as functions for the rest of the circuit (eg. writing data to the SD

card). When measuring the efficiency then, it is necessary to find what fraction of power is consumed due to the power supply exclusively.

To take this into account, a second circuit with an ATMega328p and associated circuitry was built. In this circuit, the microcontroller performed all the same tasks, except for the pulse width modulation. The power consumed by this circuit could therefore be subtracted from the total power consumed, leaving just the power consumed by the switching power supply circuitry, indicated as P_{in}.

Measuring the output power involved measuring the output voltage, squaring this value, and dividing by the output resistance. This gives

$$\text{Efficiency} = \frac{\frac{(V_{out})^2}{R_{out}}}{I_{in} \times V_{in}} \tag{5.4}$$

Using this method, the input current was measured to be 21 mA, the output voltage was measured to be 514 V, and the efficiency of the power supply was calculated to be 71%, well above the specification of 60%.

5.3 CPM Accuracy

To measure the accuracy of the radiation detector, results were compared against a commercially available Geiger counter, the GM-10 from Blackcat Systems.

Radiation comes from nuclear decay, which is a random process, causing fluctuations in background CPM radiation levels. Moreover, since a count occurs when a radioactive particle/wave hits the Geiger tube, no two Geiger tubes will necessarily record the same CPM data for the same one minute period, even if the two Geiger counters are right next to each other. In other words, differences between this device and the commercial device are expected. However, the average CPM over a long period (greater than 1 hour) for each device should be relatively close.

Figure 5.1 compares results of this device with the GM-10 over the same 30 minute period. The two devices were next to each other during testing.
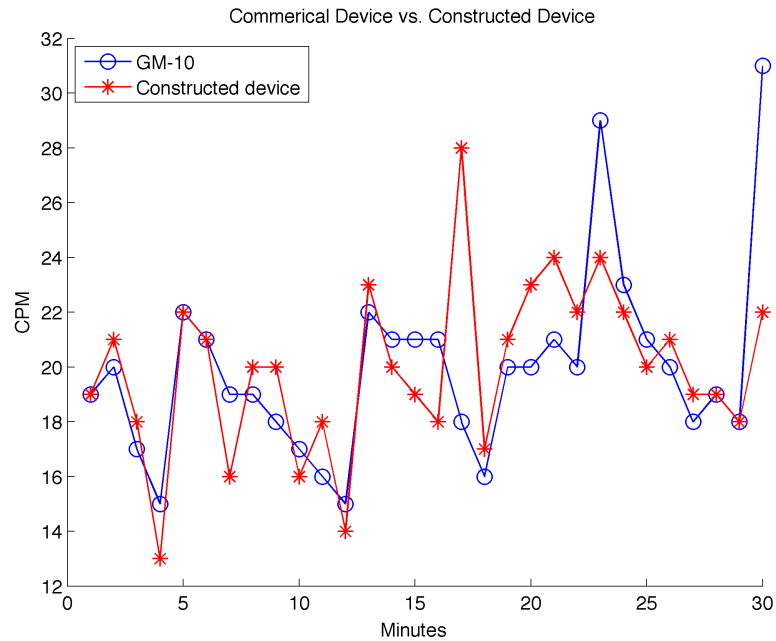
Figure 5.1. CPM data comparing the GM-10 commercial geiger counter with the designed Radiation Detector

Taking the average CPM over the 30 minute period results in values of 19.6 CPM for this device and 19.9 CPM for the GM-10. These readings correspond to 98.5% accuracy, which is well above the specification of $\geq$85%. Different time periods produce different results; therefore, the estimated device accuracy is 95–100% when the CPM data is averaged over a relatively long period (30 minutes or longer).

5.4 Overall Results

The overall results are shown below in Table 5.1. The device meets specification for all three areas: output voltage, efficiency, and accuracy. From the table it is seen that the designed device meets all specifications set forth. Continual testing showed that

Table 5.1. Project specifications and results

Specifications	Proposal	Measured	Meets specification?
Output voltage	495–605 V	514 V	Yes
Power supply efficiency	60%	71%	Yes
Count per minute accuracy	85%	96–100%	Yes

these results remained the same over time and also suggest that the design is reliable when operating for a long time period (> 1 hour).

Chapter 6

CONCLUSION

This thesis demonstrates the need for the average person to be aware of potential nuclear dangers and suggests a design for a Data Logging Radiation Detector that would potentially alert the user of nuclear radiation.

The constructed device consists of four major sections: a DC-DC boost switch mode power supply, a Geiger-Müller tube, an ATMega328p microcontroller, and a removable SD card. The device meets or exceeds all of the constraints set forth in Table 3.1. The switching power supply achievs an output voltage of 514 V and 71% efficiency, exceeding specifications. Mean CPM data agrees with a commercial Geiger counter to within 5%, also exceeding specifications.

6.1 Problems

Measuring the high output voltage from the power supply proved to be one of the most challenging aspects of the design stage. The Keithly 175 multimeter used initially calculated a root mean square reading of the voltage, while the Mastech MAS830 calculated only a peak voltage. This discrepancy slowed progress on the design as the output voltage could not be accurately determined. Gaining access to a 100 MΩscope probe allowed the output waveform to be displayed on an oscilloscope, ensuring that the power supply was operating as it was designed.

6.2 Potential Improvements

There is a range of potential functionality improvements that would directly increase the usability of this device. A few potential improvements are given below from most to least difficult:

1. Timing circuit and GPS: A timing circuit with GPS would allow each CPM recording to be transmitted with a timestamp showing the time and date. If the device is moving, it would then be possible to track its location and determine which CPM measurements are associated with certain locations.

2. Printed Circuit Board (PCB): Designing a PCB would improve the structural integrity of the device as well as reduce parasitics and provide a more professional looking package.

3. LCD: Adding an LCD would be a simple improvement that could display a running CPM average, giving the user more feedback than the current LED.

Adding these functionalities would help the Data Logging Radiation Detector be a more complete consumer level Geiger counter. These improvements would increase its appeal to the general population, hopefully making the detection of radiation more common-place and less intimidating to the average citizen in times of nuclear crisis.

REFERENCES

[1] International Atomic Energy Agency. "Nuclear Power Worldwide: Status and Outlook", IAEA Press Releases, 23 October 2007.
http://www.iaea.org/newscenter/pressreleases/2007/prn200719.html

[2] Schneider, Mycle. "2008 World nuclear industry status report: Global nuclear power," *Bulletin of the Atomic Scientists*, 16 September 2008,
http://www.thebulletin.org/web-edition/reports/2008-world-nuclear-industry-status-report/2008-world-nuclear-industry-status-rep

[3] Novak, Stanislav; Podest, Milan. "Nuclear power plant aging and life extension: Safety aspects," *International Atomic Energy Agency Bulletin*, April 1987.

[4] Wald, Matthew. "Nuclear 'Renaissance' Is Short on Largess", *The New York Times*, 7 December 2010. http://green.blogs.nytimes.com/2010/12/07/nuclear-renaissance-is-short-on-largess/

[5] Butler, Decan. "Reactors, residents, and risk." *Nature*, 21 April 2011.
http://www.nature.com/news/2011/110421/full/472400a.html

[6] Brumfiel, Geoffrey. "Directly comparing Fukushima to Chernobyl." *Nature* 07 September 2011.
http://blogs.nature.com/news/2011/09/directly_comparing_fukushima_t.html

[7] World Nuclear Association. "Fukushima Accident 2011". April 2012.
http://www.world-nuclear.org/info/fukushima_accident_inf129.html

[8] Kopytoff, Verne G. "Japan's Nuclear Crisis Causes Run on Radiation Detectors", *The New York Times*. 21 March 2011.
http://www.nytimes.com/2011/03/22/business/22geiger.html

[9] Alpeyev, Pavel. "Japan Geiger Counter Demand After Fukushima Earthquake Means Buyer Beware", *Bloomberg* 14 Jul 2011.
http://www.bloomberg.com/news/2011-07-15/geiger-counters-sell-out-in-post-fukushima-japan.html

[10] Tabuchi, Hiroko. "Japan Panel Cites Failure in Tsunami," *The New York Times*, 26 December 2011. http://www.nytimes.com/2011/12/27/world/asia/report-condemns-japans-response-to-nuclear-accident.html

[11] Roan, Shari. "Possible health effects of nuclear crisis", *The Los Angeles Times* 16 March 2011. http://articles.latimes.com/2011/mar/16/health/la-he-japan-quake-radiation-20110316

[12] World Nuclear Association. "Nuclear Radiation and Health Effects". November 2011. http://www.world-nuclear.org/info/inf05.html

[13] Karam, Andrew. "What Those Fukushima Radiation Counts Really Mean: Analysis", *Popular Mechanics*. May 10, 2011. http://www.popularmechanics.com/science/energy/nuclear/what-those-fukushima-radiation-counts-really-mean-analysis-5719140

[14] Cartlidge, Edwin. "Fukushima maps identify radiation hot spots." *Nature* 14 November 2011. http://www.nature.com/news/fukushima-maps-identify-radiation-hot-spots-1.9355#/b1

[15] Centronic Corporation. *Geiger Müller Tubes.* http://www.centronic.co.uk/downloads/Geiger_Tube_theory.pdf

[16] Abraham Pressman, *Switching Power Supply Design*. McGraw Hill: New York, 3rd Ed. 2009.

[17] Ravindra Ambatipudi, *Low Cost Boost Converters Using LM3578A*. National Semiconductor Application Note 1066. November 1999.

Appendix A

PROJECT PROPOSAL

A.1 Details

This project aims to add functionality to Professor Eason's scientific ballooning module. In particular, a radiation detector will be added to detect the presence of alpha, beta, and gamma radiation. By generating a high voltage across the Geiger tube, it is possible to detect the random collisions of alpha particles, beta particles, and gamma rays. (Normal radiation levels are approximately 2.4 millisievert/year or 1.09×10^{-7} SV/hour. This translates to around 25 counts per minute or cpm.) Upon detection, a pulse of current will be sent to the microprocessor which will then process the data and produce a digital output.

A.2 Inputs/Outputs

Inputs to the project will be a DC voltage for the microprocessor and the Geiger Tube. Output will be a digital signal from the microprocessor.

A.3 Specifications

The input to the power supply will be a DC voltage between 3-12 V and the output of will be 550 V $\pm$ 10%. Overall power supply efficiency should be greater than or equal to 60%. The circuit should be able to measure background radiation to within $\pm$50% of normal levels.

Appendix B

SCHEMATIC

A complete project schematic can be found on the next page.

Joseph Record, Brian Grant

TITLE: Geiger_Counter_Final

Document Number:

REV: 1.0

Date: 2/23/2012 8:55:42 AM

Sheet: 1/1

CODE LISTING

main.c

```
 1  // Geiger Counter with SD Card Output
    // Senior Project - Brian Grant & Joseph Record
    // PWM for Power Supply, LED Status, SD Card Output
    // Using low level SD card routines adaped from Roland Reigel's
        project "MMC/SD/SDHC Card Library"
    // http://www.roland-riegel.de/sd-reader/index.html
 6
    #include <string.h>
    #include <avr/pgmspace.h>
    #include <stdlib.h>
    #include <stdio.h>
11  #include <avr/io.h>
    #include <avr/interrupt.h>
    #include <util/delay.h>
    #include "fat.h"
    #include "fat_config.h"
16  #include "partition.h"
    #include "sd_raw.h"
    #include "sd_raw_config.h"

    #define sbi(var, mask)    ((var) |= (uint8_t)(1 << mask))
21  #define cbi(var, mask)    ((var) &= (uint8_t)˜(1 << mask))
    #define STATUS_LED 3
    #define ERROR_LED 2

    void pwm_init(void);
26  void cpm_init(void);
    void led_init(void);
    uint8_t exit_check(void);
    uint8_t adc_read(uint8_t adc_num);
    static struct fat_file_struct* open_file_in_dir(struct
        fat_fs_struct* fs, struct fat_dir_struct* dd, const char* name);
31  static uint8_t find_file_in_dir(struct fat_fs_struct* fs, struct
        fat_dir_struct* dd, const char* name, struct
        fat_dir_entry_struct* dir_entry);

    uint16_t cpm = 0;      // count per minute rolling storage
    uint16_t cpm_final = 0;   // count per minute to be written to SD
        card
    uint8_t geiger_flag = 0;  // radiation detection flag
36  uint8_t minute_flag = 0;  // minute expiry flag

    int main(void)
    {
      char buffer[10];
```

```c
41   uint8_t buffer_len = 0;
     uint8_t first_write = 1;

     pwm_init(); // setup pwm for power supply
     cpm_init(); // setup 1 min timer for cpm
46   led_init(); // setup status LEDs and geiger trigger

     // initialize SD card
     if(!sd_raw_init()) sbi(PORTC, ERROR_LED); // SD initialization
         failed

51   // open first partition
     struct partition_struct* partition = partition_open(sd_raw_read,
         sd_raw_read_interval, sd_raw_write, sd_raw_write_interval, 0);
     if(!partition) sbi(PORTC, ERROR_LED); // opening partition failed

     // open file system
56   struct fat_fs_struct* fs = fat_open(partition);
     if(!fs) sbi(PORTC, ERROR_LED); // opening filesystem failed

     // open root directory
     struct fat_dir_entry_struct directory;
61   fat_get_dir_entry_of_path(fs, "/", &directory);
     struct fat_dir_struct* dd = fat_open_dir(fs, &directory);
     if(!dd) sbi(PORTC, ERROR_LED); // opening root directory failed

     // create file
66   struct fat_dir_entry_struct file_entry;
     char file_name[8] = {'c','p','m','.','t','x','t','\0'};
     if(find_file_in_dir(fs, dd, file_name, &file_entry)) { // if file
         exists, erase it
       if(!fat_delete_file(fs, &file_entry)) sbi(PORTC, ERROR_LED); //
           error deleting file
       if(!sd_raw_sync()) sbi(PORTC, ERROR_LED); // error syncing disk
71   }
     if(!fat_create_file(dd, file_name, &file_entry)) sbi(PORTC,
         ERROR_LED); // error creating file
     if(!sd_raw_sync()) sbi(PORTC, ERROR_LED); // error syncing disk

     // open created file
76   struct fat_file_struct* fd = open_file_in_dir(fs, dd, file_name);
     if(!fd) sbi(PORTC, ERROR_LED);  // error opening file

     while (adc_read(0) > 128) {   // check eject/done jumper
       OCR0A = ~adc_read(1);   // adjust duty cycle based on feedback
           voltage
81     if (geiger_flag) {      // check for particle detected
         sbi(PORTC, STATUS_LED); // turn on status LED
         _delay_ms(100);     // hold LED high long enough for human to
             see
         cbi(PORTC, STATUS_LED); // turn off status LED
         geiger_flag = 0;    // clear geiger flag
86     }
```

```
      if (minute_flag) {                    // check for minute expiry –
         write cpm to sd card
        if (first_write) {                   // check for first write since
           bootup
         sprintf(buffer,"%d",cpm_final);      // convert cpm varaible
            to string (first write without leading comma)
         first_write = 0;                    // clear first write flag
91       }
        else sprintf(buffer,",%d",cpm_final);   // convert cpm
           varaible to string
        buffer_len = strlen(buffer);         // get length of cpm string
        if(fat_write_file(fd, (uint8_t*) buffer, buffer_len) !=
           buffer_len) sbi(PORTC, ERROR_LED); // error writing to file
        if(!sd_raw_sync()) sbi(PORTC, ERROR_LED); // flush SD write
           buffer
96      cpm_final = 0;                       // clear cpm
        minute_flag = 0;                     // clear minute flag
      }
    }

101 fat_close_file(fd);        // close file
    fat_close_dir(dd);         // close directory
    fat_close(fs);            // close file system
    partition_close(partition);   // close partition
    sbi(PORTC, STATUS_LED);      // indicate exit process has completed
106 while (1) OCR0A = ~adc_read(1); // adjust duty cycle based on
       feedback voltage
      return 0;
}

ISR (INT0_vect)      // geiger tube trigger
111 {
    cpm++;           // increment rolling cpm
    geiger_flag = 1;  // set geiger flag to cause LED to light
}

116 ISR (TIMER1_COMPA_vect) // one minute timer trigger
    {
    cpm_final = cpm;  // save current cpm
    cpm = 0;         // clear rolling cpm
    minute_flag = 1;  // set minute expiry flag to cause write to SD
       card
121 }

    void pwm_init(void)             // setup pwm for power supply
    {
    DDRD |= (1 << DDD6);          // set PD6 as an output
126   OCR0A = 153;                // set PWM for 60% duty cycle
      TCCR0A |= (1 << COM0A1);        // set none-inverting mode
      TCCR0A |= (1 << WGM01) | (1 << WGM00);  // set fast PWM Mode
      TCCR0B |= (1 << CS00);          // set prescaler to 1 and start
         PWM
    }
131
```

```
void cpm_init(void)              // setup 1 min timer for cpm
{
  OCR1A = 0xE4E1;                // compare value = (1MHz/1024)*60sec -
      1
    TCCR1B |= (1 << WGM12);        // mode 4, CTC on OCR1A
    TIMSK1 |= (1 << OCIE1A);        // set interrupt on compare
        match
    TCCR1B |= (1 << CS12) | (1 << CS10);  // set prescaler to 1024
        and start the timer
}

void led_init(void)            // setup status LEDs and geiger trigger
{
  DDRC |= (1 << DDC2) | (1 << DDC3);  // set PC2 & PC3 as outputs
  EICRA |= (1 << ISC01);          // trigger on falling edge of INT0
  EIMSK |= (1 << INT0);          // enable INT0
  sei();                  // enable global interrupts
}

uint8_t adc_read(uint8_t adc_num)
{
  ADMUX = adc_num;             // read specified ADC
    ADMUX |= (1 << REFS0);          // set AVcc as the reference
    ADMUX |= (1 << ADLAR);          // set 8 bit resolution
    ADCSRA |= (1 << ADPS1) | (1 << ADPS0);  // set presaler to 8
  ADCSRA |= (1 << ADEN);          // enable the ADC
    ADCSRA |= (1 << ADSC);          // single conversion mode
  while(ADCSRA & (1 << ADSC));      // wait until conversion is
      complete
    return ADCH;
}

struct fat_file_struct* open_file_in_dir(struct fat_fs_struct* fs,
    struct fat_dir_struct* dd, const char* name)
{
    struct fat_dir_entry_struct file_entry;
    if(!find_file_in_dir(fs, dd, name, &file_entry)) return 0;  //
        check that file exists
    return fat_open_file(fs, &file_entry);          // open file
}

uint8_t find_file_in_dir(struct fat_fs_struct* fs, struct
    fat_dir_struct* dd, const char* name, struct
    fat_dir_entry_struct* dir_entry)
{
    while(fat_read_dir(dd, dir_entry)) {        // scan through
        directory
        if(strcmp(dir_entry->long_name, name) == 0) { // look for
            file name match
            fat_reset_dir(dd);
            return 1;
        }
    }
    return 0;
```

```
176     }
```

BIOGRAPHY OF THE AUTHOR

Joseph Record was born in Augusta, Maine on January 18, 1990. He received his high school diploma from Cony High School in Augusta in 2008.

In the fall of 2008, he was enrolled for undergraduate study in Electrical Engineering at the University of Maine. He has served as an NSF REU research assistant in Professor Mauricio da Cunha's Microwave Acoustics Labratory. His current research interests include semiconductor devices, VLSI design and layout, and microelectronics. His interests include reading (preferably Bill Bryson, Christopher Hitchens, and other assorted non-fiction), hiking, chess, table tennis, and cycling.

He is a candidate for the Bachelor of Science degree with Honors in Electrical Engineering from the University of Maine in May 2012.